TU/e EINDHOVEN UNIVERSITY OF TECHNOLOGY

Characterization of the Dielectric Properties of Commercially Available Low-loss UV-curable Resins from 60 GHz to 90 GHz

Citation for published version (APA):
Escobari Vargas, P., Meyer, E., Chiappini, F., Garufo, A., Monni, S., Johannsen, U., & Reniers, A. C. F. (2022). Characterization of the Dielectric Properties of Commercially Available Low-loss UV-curable Resins from 60 GHz to 90 GHz. In *2022 52nd European Microwave Conference (EuMC)* (pp. 278-281). Article 9924501 Institute of Electrical and Electronics Engineers. https://doi.org/10.23919/EuMC54642.2022.9924501

Document license:
Unspecified

DOI:
10.23919/EuMC54642.2022.9924501

Document status and date:
Published: 31/10/2022

Document Version:
Accepted manuscript including changes made at the peer-review stage

Please check the document version of this publication:

• A submitted manuscript is the version of the article upon submission and before peer-review. There can be important differences between the submitted version and the official published version of record. People interested in the research are advised to contact the author for the final version of the publication, or visit the DOI to the publisher's website.
• The final author version and the galley proof are versions of the publication after peer review.
• The final published version features the final layout of the paper including the volume, issue and page numbers.

Link to publication

General rights
Copyright and moral rights for the publications made accessible in the public portal are retained by the authors and/or other copyright owners and it is a condition of accessing publications that users recognise and abide by the legal requirements associated with these rights.

• Users may download and print one copy of any publication from the public portal for the purpose of private study or research.
• You may not further distribute the material or use it for any profit-making activity or commercial gain
• You may freely distribute the URL identifying the publication in the public portal.

If the publication is distributed under the terms of Article 25fa of the Dutch Copyright Act, indicated by the “Taverne” license above, please follow below link for the End User Agreement:

www.tue.nl/taverne

Take down policy
If you believe that this document breaches copyright please contact us at:

openaccess@tue.nl

providing details and we will investigate your claim.

Download date: 21. Mar. 2025

Characterization of the Dielectric Properties of Commercially Available Low-loss UV-curable Resins from 60 GHz to 90 GHz

P. Escobari Vargas[#1,2], E. Meyer[1], F. Chiappini[2,3], A. Garufo[3], S. Monni[2,3], U. Johannsen[1], A. C. F. Reniers[1,4]

[1]Technical University of Eindhoven, The Netherlands

[2]Chip Integration Technology Center CITC, Nijmegen, The Netherlands

[3]Netherlands Organization for Applied Scientific Research TNO

[4]Antennex B.V., Eindhoven, The Netherlands

[#]p.a.escobari.vargas@tue.nl

***Abstract* — In this paper, two important dielectric properties, the relative permittivity and the loss tangent of a new commercially available UV-curable SLA resin sample are determined. The characterization of the dielectric material is performed in the millimetre-wave range using an open-cavity Fabry-Pérot resonator. According to the manufacturer's data sheet, this ultra low-loss photoresist material, optimised for advanced electronic applications, has a relative permittivity of 2.6 and a loss tangent of 0.003, both at 10 GHz. First, the accuracy of the Fabry-Pérot open-cavity resonator was determined using a reference material called Rexolite. Then, the new dielectric material was measured in a frequency band from 60 GHz to 90 GHz. The results show that the new commercial resin sample has a relative permittivity of 2.59 and a loss tangent of 0.0031 at 71.8 GHz.**

***Keywords* — Loss tangent, material characterization, millimeter wave (mmWave), Fabry-Pérot open-cavity resonator, relative permittivity, SLA resin.**

I. Introduction

In recent years, the popularity of additive manufacturing (AM) in electronics manufacturing has grown. Thanks to the performance improvement, AM is becoming increasingly interesting for RF applications as a potential alternative to conventional mold compound-based manufacturing processes. The combination of AM and electronic device integration is called 3D printed structural electronics (3DPSE) [1]. 3DPSE has important advantages like free form factors, reduced size, rapid prototyping, light weight, varied material combination and costs saving [2]. These advantages allow the production of fully integrated and embedded electronic systems. Several 3D printing technologies, such as Fused Filament Fabrication (FFF), Digital Light Process (DLP), Stereolithography (SLA) and others, have been tested for 3DPSE. Multiple articles, for example [3], [4] and [5], have studied the dielectric properties of polymers used exclusively in FFF up to 12 GHz [4]. Fewer studies have characterized negative photoresist resins like in [6], [7] and [8]. These studies use commercial measurement tools to obtain values for the relative permittivity and loss tangent at millimeter wave (mmWave) and THz frequencies. Both [6] and [7] use time domain spectroscopy. In [7], the characterization of a Formlabs SLA resin, Tough FLTOTL04, resulted in a relative permittivity of 2.8 at 100 GHz down to 2.35 at 2 THz and a loss tangent of 0.021 at 100 GHz up to 0.103 at 2 THz. The mechanical and thermal performance is characterized and shown in the supplier data sheet [9].

SLA 3D printing technologies have clear advantages compared to FFF: the high printing velocity, printing resolution, smooth surfaces and small form factors make it an appealing printing technology for 3DPSE. Several works utilize SLA 3D printers and commercial UV-cured resins. In [10], a metal-coated 3D printed horn antenna and a metal-coated 3D printed corrugated mirror are tested at 92.5 GHz and 140 GHz, respectively. In [11], a 3D printed straight waveguide and a diagonal horn antenna are coated using copper and tested in the WR-3.4 band (from 220 GHz to 330 GHz). The comparison between this antenna and its metallic counterpart show similar co-polarization, directivity and side-lobes performance.

Another example of 3DPSE is presented in [12], where a 24 GHz antenna for miniaturized FMCW radar was 3D printed using SLA technology. The half-wavelength dipole antenna is compared to simulations showing a difference in gain of 2 dB at 22 GHz. In [12], measurements of the relative permittivity of the commercial resin are obtained by using a cavity resonator at the X and Ka frequency bands. The results show a relative permittivity of 2.74 at 24 GHz. Most of the cited works show high shape versatility and printing resolutions up to 50 μm [12], making this technology one of the first options for 3DPSE for mmWave and THz applications. None of these works used low-loss UV-curable resins now available on the market. For example, the UV-curable photopolymer in [13], shows a data sheet dissipation factor as low as 0.0046 at 10 GHz, which can be very advantageous in reducing the loss of 3DPSE components.

For RF components and antennas, accurate characterization of the substrate material is of paramount importance as input for the design process and correct performance prediction. This is even more important as the operating frequency increases. In this work a sample of a low-loss commercial resin suitable for SLA-based 3D printing is characterized for 60-90 GHz, which means a wavelength of 3.3-5 mm. A rexolite sample is

used as benchmark material to verify, calibrate and determine the accuracy of the Fabry-Pérot open-cavity resonator.

This paper is organized as follows. The measurement setup is detailed in Section II, the sample preparation is explained in Section III and the results and discussions are presented in Section IV.

II. Measurement Set-up

A. Fabry-Pérot Open-Cavity Resonator

A Fabry-Pérot resonator with an open cavity was designed and assembled at the Eindhoven University of Technology, see Fig. 1. The Fabry-Pérot open-cavity resonator consists of two spherical concave mirrors positioned on two motor stages (M-413.32S) [14]. With the help of these motor stages, the mirrors can be adjusted to different focal lengths, e.g. near-focal, near-confocal or near-concentric.

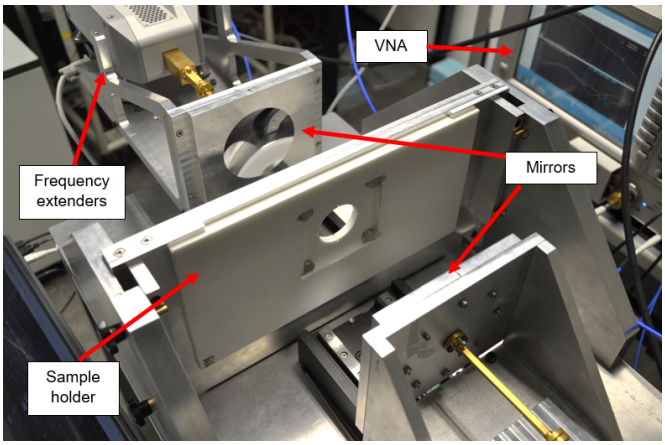

Fig. 1. Perspective view of the Fabry-Pérot open-cavity resonator.

A Vector Network Analyzer (VNA) with frequency extenders is used to excite the electromagnetic field in the open cavity as shown in Fig. 2.

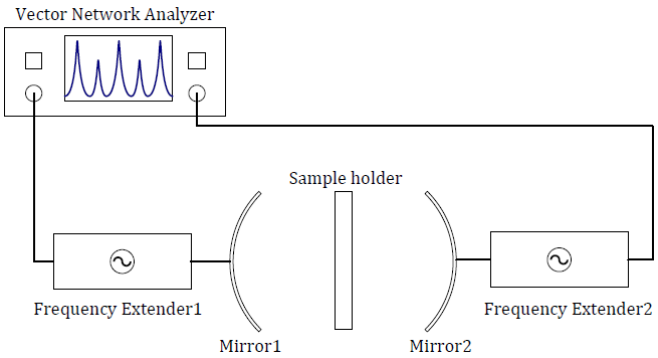

Fig. 2. Illustration of the Fabry-Pérot open-cavity resonator, VNA and frequency extenders.

In the centre of the cavity, a sample holder for the dielectric material is placed. This dielectric material holder can hold dielectric samples with a minimum length $\times$ width of 75 mm $\times$ 75 mm and a thickness varying from 10 μm up to 3000 μm, which depends on the frequency range.

In this Fabry-Pérot open resonator, a near-concentric configuration is used to insure stability, avoid the propagation of additional modes and increase the Q-factor of the resonator.

As explained in [15], the fundamental ($\text{TEM}_{0,0,q}$) mode can be symmetrical ($q = 2$) or antisymmetrical ($q = 1$). From both modes the relative permittivity and the loss tangent can be determined, whereby, depending on the relative permittivity, either the symmetric or the antisymmetric mode gives the most accurate result [16].

Inside the open resonator, the fundamental ($\text{TEM}_{0,0,q}$) mode propagates with a Gaussian profile. This Gaussian beam presents a beam waist that illuminates the dielectric sample in the center of the cavity and defines the size of the analyzed spot. The beam waist size is determined by the radius of curvature of the mirrors and the distance between the mirrors. In the Fabry-Pérot open-cavity resonator used for this research, the beam waist's diameter is about 22 mm over the entire frequency band, from 60 GHz to 90 GHz. This specified beam waist size corresponds to 95% of the total energy of the Gaussian beam.

The relative permittivity and the loss tangent are determined by first performing a measurement without a sample, i.e. with an unloaded cavity, and then a measurement with a sample, i.e. with a loaded cavity. The data obtained is processed using an algorithm based on the equations discussed in [17].

B. Measurement Protocol

Using the Fabry-Pérot open-cavity resonator described in II-A, a dielectric material is characterized over a frequency band from 60 GHz to 90 GHz, which is subdivided into 10 sub-frequency bands for a more detailed analysis. The measurement protocol is:

1) Set the distance between the mirrors according to the sample thickness, the sub-frequency band to be analyzed and the number of half-wavelengths between the mirrors (q).
2) Extract and save two S-parameter traces of the unloaded resonator from the VNA, the S_{12} and S_{21}.
3) Place the dielectric material holder with the sample as accurately as possible in the centre of the resonator. The area under analysis is an uncovered circle of 4 cm diameter, see Fig. 1
4) Measure a second set of S_{12} and S_{21} of the loaded resonator with the same VNA settings.
5) Determine the relative permittivity and loss tangent of the dielectric material by processing the resonant frequency shift of the S-parameters and the difference of the Q-factors of the resonator with the equations discussed in [17].
6) Compare the results for the relative permittivity and loss tangent obtained using S_{12} and S_{21} to discard measurements affected by variations in dielectric material placement.
7) Repeat the procedure for all sub-frequency bands.

According to the assumptions in [17], some constraints on the dielectric sample conditions have to be considered: constant thickness along the analyzed site, no deformation (warpage), 5 cm or more in diameter, 100 μm - 1 mm in thickness. Another condition for the setup is that the dielectric material must be placed exactly in the centre of the resonator.

III. Sample Preparation

A. UV-curable Resin Samples

The material under test is the ultra low dissipation factor dielectric resin PRO14371 supplied by Arkema as part of its N3XTDIMENSION® product line [18]. To produce a resin sample, the liquid resin is pressed using two quartz plates and then cured for 30 minutes in a UV chamber. The UV chamber, "Next Dent LC -3DPrint Box", has 12 UV lamps to ensure that the sample is illuminated from all sides. This process is chosen to limit surface roughness and warpage, but can also introduce some air bubbles into the samples.

After curing, measurements of the thickness are taken at several points on the samples, as shown in Fig. 3.

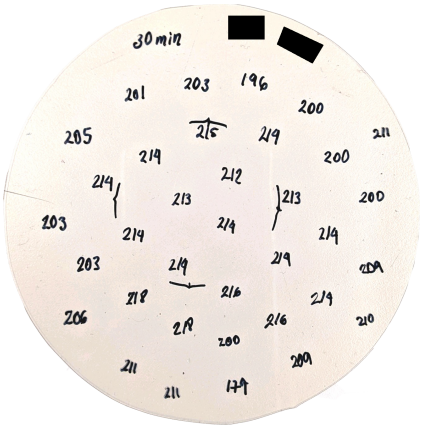

Fig. 3. Thickness measurements of a 30-minutes UV-cured resin sample.

The area to be measured is a selected circle with a diameter of 4 cm, which has minimal warpage, thickness variations and air bubbles.

B. Rexolite Sample

The rexolite sample used as reference material is a sheet of 8 cm $\times$ 10 cm and a thickness of 490 μm. The thickness is also measured at several points on the sample and along the analyzed points with a thickness gauge of 1 μm resolution.

According to [19], the Rexolite's relative permittivity measured at 76.5 GHz is 2.529 and the loss tangent is 0.00063.

IV. Results and Discussion

Using the measurement protocol explained in II-B, several measurements are made for the resin and the rexolite sample. The measurements are carried out under the assumption that both samples have a negligible content of air bubbles, surface roughness and warpage.

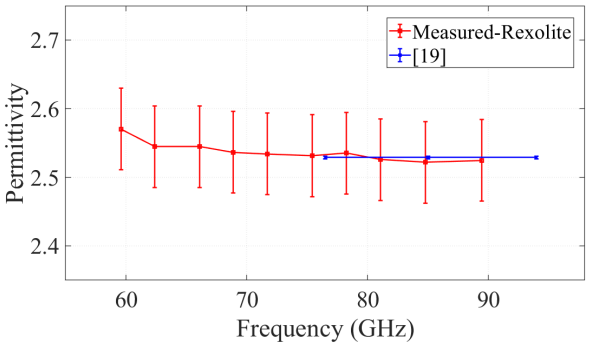

Fig. 4. Measurement results of the relative permittivity of Rexolite.

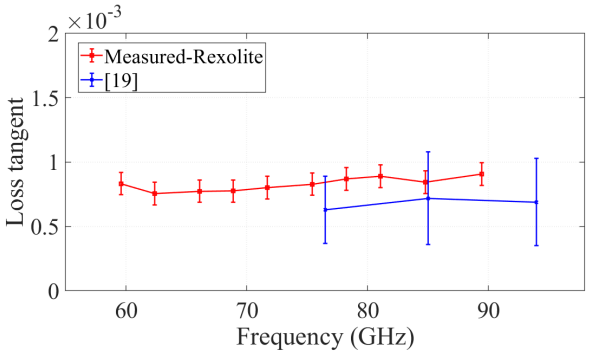

Fig. 5. Measurement results of the loss tangent of Rexolite.

The final results are shown in Fig. 4 and in Fig. 5, where the measurements of the rexolite using the open resonator setup show comparable results to those published by [19].

In Figs. 4 and 5, the bars at each measured point indicate the measurement uncertainty, calculated according to [20], where the combined uncertainty is the root sum of squares of the independent uncertainties due to: system's repeatability and thickness variations. The latter comprises, in this case, more than 90% of the final uncertainty.

The UV-cured resin is also characterized and the results are shown in Fig. 6, a dielectric constant of 2.59 and a loss tangent of 0.00309 at 71.8 GHz are found. The resin's permittivity and loss tangent show a stable behavior along the studied frequency band.

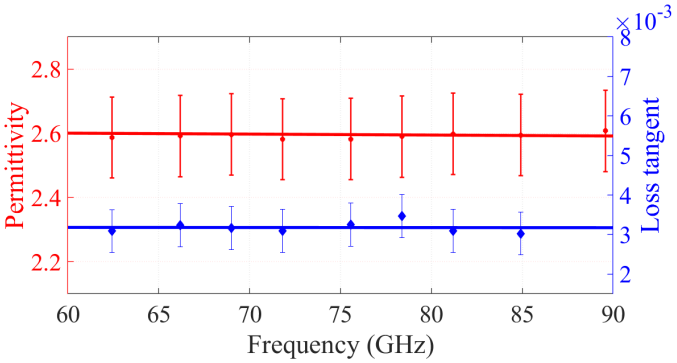

Fig. 6. Least-square fitting of the relative permittivity and loss tangent of the resin sample.

In Fig. 6, a least-square linear fitting is done over the measurements of the relative permittivity and loss tangent of the resin sample. This approximation shows that the relative permittivity and loss tangent meet the values specified by the manufacturer at 10 GHz, a relative permittivity of 2.6 and a loss tangent of 0.003.

The resin sample measured in this work, is an improved and optimized photopolymer for electronics applications, compared to the commercial resin used in [7], the losses are an order of magnitude lower at high frequency bands, which makes it very suitable for mmWave applications.

V. Conclusion

A sample of the ultra low-loss UV-curable PRO14731 resin, is characterized from 60 GHz to 90 GHz using a Fabry-Pérot open-cavity resonator. Using the measurement protocol proposed in this work, a relative permittivity of 2.59 and a loss tangent of 0.0031 were obtained at 71.8 GHz. The combined final uncertainty includes the uncertainties due to the irregularities of the sample. By a linear least-squares fit over the measurements, an estimate of the relative permittivity and loss tangent over the analyzed frequency band can be found, showing agreement with the manufacturer's specifications. The measured relative permittivity and loss tangent show a stable behaviour in the investigated frequency band, these values can be used as an input in the design of 3D SLA printed electronics for mmWave applications.

Acknowledgment

The authors want to acknowledge the support of TNO Radar Technology and TNO Holst Centre for providing and fabricate the material samples used in this work. The authors thank the cooperation and support of Sartomer's N3xtDimension product line, based in Exton, Pennsylvania, USA. The authors also express special appreciation to Rob Hendriks and Darragh Walsh for providing support and access to specialized equipment during the development of this work. Finally, the authors acknowledge the support of Antennex B.V. in providing access to the Fabry-Pérot resonator.

References

[1] H. H. H. Maalderink, F. B. J. Bruning, M. M. R. de Schipper, J. J. J. van der Werff, W. W. C. Germs, J. J. C. Remmers, and E. R. Meinders, "3D Printed structural electronics: embedding and connecting electronic components into freeform electronic devices," *Plastics, Rubber and Composites*, vol. 47, no. 1, pp. 35–41, 2018. [Online]. Available: https://doi.org/10.1080/14658011.2017.1418165

[2] D. V. Baker, C. Bao, and W. S. Kim, "Highly Conductive 3D Printable Materials for 3D Structural Electronics," *ACS Applied Electronic Materials*, vol. 3, no. 6, pp. 2423–2433, 2021.

[3] P. Veselý, T. Tichý, O. Šefl, and E. Horynová, "Evaluation of dielectric properties of 3D printed objects based on printing resolution," *IOP Conference Series: Materials Science and Engineering*, vol. 461, p. 012091, dec 2018. [Online]. Available: https://doi.org/10.1088/1757-899x/461/1/012091

[4] A. Goulas, S. Zhang, D. A. Cadman, J. Järveläinen, V. Mylläri, W. G. Whittow, J. Y. C. Vardaxoglou, and D. S. Engstrøm, "The Impact of 3D Printing Process Parameters on the Dielectric Properties of High Permittivity Composites," *Designs*, vol. 3, no. 4, 2019. [Online]. Available: https://www.mdpi.com/2411-9660/3/4/50

[5] D. Kalaš, K. Šíma, P. Kadlec, R. Polanský, R. Soukup, J. Řeboun, and A. Hamáček, "FFF 3D Printing in Electronic Applications: Dielectric and Thermal Properties of Selected Polymers," *Polymers*, vol. 13, no. 21, 2021. [Online]. Available: https://www.mdpi.com/2073-4360/13/21/3702

[6] N. Ghalichechian and K. Sertel, "Permittivity and Loss Characterization of SU-8 Films for mmW and Terahertz Applications," *IEEE Antennas and Wireless Propagation Letters*, vol. 14, pp. 723–726, 2015.

[7] S. Sahin, N. Nahar, and K. Sertel, "Dielectric Properties of Low-Loss Polymers for mmW and THz Applications," *J Infrared Milli Terahz Waves*, vol. 40, p. 557–573, march 2019. [Online]. Available: https://doi.org/10.1007/s10762-019-00584-2

[8] Y. Fu, W. Li, M. Xu, C. Wang, L. Zhang, and G. Zhang, "Dielectric Properties and 3D-Printing Feasibility of UV-Curable Resin/Micron Ceramic Filler Composites," *Hindawi, Advances in Polymer Technology*, vol. 2022, no. 9483642, pp. 1–14, 2022.

[9] (2018) Material datasheet: Tough resin. [Online]. Available: https://formlabs-media.formlabs.com/datasheets/Tough_Technical.pdf

[10] A. Macor, E. de Rijk, S. Alberti, T. Goodman, and J.-P. Ansermet, "Note: Three-dimensional stereolithography for millimeter wave and terahertz applications," *Review of Scientific Instruments*, vol. 83, no. 4, p. 046103, 2012. [Online]. Available: https://doi.org/10.1063/1.3701738

[11] A. von Bieren, E. de Rijk, J.-P. Ansermet, and A. Macor, "Monolithic metal-coated plastic components for mm-wave applications," in *2014 39th International Conference on Infrared, Millimeter, and Terahertz waves (IRMMW-THz)*, 2014, pp. 1–2.

[12] C. Yepes, E. Gandini, R. v. Dijk, F. Bruning, H. Maalderink, S. Monni, and F. E. van Vliet, "Additive manufactured antenna in mixed material technology for 24 ghz fmcw miniaturized radar," in *2018 15th European Radar Conference (EuRAD)*, 2018, pp. 397–400.

[13] (2021) Material datasheet: Radix low-loss resin. [Online]. Available: https://3dfortify.com/wp-content/uploads/2021/12/..
..Radix-2.8dk-Printable-Dielectric-Data-Sheet.pdf

[14] (2020) Physik Instrumente. [Online]. Available: https://www.physikinstrumente.store/eu/m-413.32s/

[15] G. Federico, A. Reniers, A. Roc'h, L. Bronckers, and H. Visser, "Complex permittivity measurements with a low cost parabolic resonant cavity," in *The Loughborough Antennas Propagation Conference (LAPC 2018)*, 2018, pp. 1–6.

[16] A. L. Cullen and P. K. Yu, "The accurate measurement of permittivity by means of an open resonator," *Proceedings of the Royal Society of London. Series A, Mathematical and Physical Sciences*, vol. 325, no. 1563, pp. 493–509, 1971. [Online]. Available: http://www.jstor.org/stable/77945

[17] A. L. Cullen and P. K. Yu, "Measurement of Permittivity by Jeans of an Open Resonator," *Proceedings of the Royal Society of London. Series A, Mathematical and Physical Sciences*, vol. 380, no. 1778, pp. 49–71, 1982.

[18] (2021) Sartomer Ultra low-loss resin. [Online]. Available: https://www.sartomer.com/en/media/news/non-global/sites/sartomer/..
..2021/Sartomer-introduces-ultra-low-loss-resins/

[19] G. Friedsam, "Precision Free-Space Measurements of Complex Permittivity of Polymers in the W-Band," *IEEE MTT-S Digest*, pp. 1351–1354, 1997.

[20] (1994) NIST Uncertainty Guidelines. [Online]. Available: https://emtoolbox.nist.gov/Publications/NISTTechnicalNote1297s.pdf